NeuroImage: Clinical 10 (2016) 27–35

Contents lists available at ScienceDirect

NeuroImage: Clinical

journal homepage: www.elsevier.com/locate/ynicl

Relationship between the anterior forebrain mesocircuit and the default mode network in the structural bases of disorders of consciousness

Nicholas D. Lant[a], Laura E. Gonzalez-Lara[a], Adrian M. Owen[a], Davinia Fernández-Espejo[a,b,*]

[a]The Brain and Mind Institute, The University of Western Ontario, London, ON N6A 5B7, Canada
[b]School of Psychology, University of Birmingham, Birmingham, B15 2TT, UK

ARTICLE INFO

Article history:
Received 28 August 2015
Received in revised form 22 October 2015
Accepted 7 November 2015
Available online 10 November 2015

Keywords:
Disorders of consciousness
Default mode network
Thalamus
Basal ganglia
Anterior forebrain mesocircuit
Precuneus
DTI
Tractography
White matter
Traumatic brain injury
Hypoxic–ischemic brain injury
Vegetative state
Minimally conscious state

ABSTRACT

The specific neural bases of disorders of consciousness (DOC) are still not well understood. Some studies have suggested that functional and structural impairments in the default mode network may play a role in explaining these disorders. In contrast, others have proposed that dysfunctions in the anterior forebrain mesocircuit involving striatum, globus pallidus, and thalamus may be the main underlying mechanism. Here, we provide the first report of structural integrity of fiber tracts connecting the nodes of the mesocircuit and the default mode network in 8 patients with DOC. We found evidence of significant damage to subcortico-cortical and cortico-cortical fibers, which were more severe in vegetative state patients and correlated with clinical severity as determined by Coma Recovery Scale—Revised (CRS-R) scores. In contrast, fiber tracts interconnecting subcortical nodes were not significantly impaired. Lastly, we found significant damage in all fiber tracts connecting the precuneus with cortical and subcortical areas. Our results suggest a strong relationship between the default mode network – and most importantly the precuneus – and the anterior forebrain mesocircuit in the neural basis of the DOC.

1. Introduction

Disorders of consciousness (DOC) can result from a variety of focal and widespread patterns of injuries but exact pathological taxonomies for diagnosis have not yet been developed (Giacino et al., 2014). Nevertheless, impairments in thalamocortical and frontoparietal networks appear as consistent findings in recent neuroimaging studies (Cauda et al., 2009; Crone et al., 2013, 2015; Hannawi et al., 2015). Specifically, DOC patients show functional (Cauda et al., 2009; Soddu et al., 2012; Vanhaudenhuyse et al., 2010), metabolic (Laureys et al., 1999) and structural (Fernandez-Espejo et al., 2012) disconnections within thalamocortical and cortico-cortical regions of the default mode network (DMN), which are correlated with clinical severity (Fernandez-Espejo et al., 2012; Vanhaudenhuyse et al., 2010). A recent study has further stressed the importance of thalamocortical connections by revealing specific patterns of impaired metabolic activity in the anterior forebrain mesocircuit (Fridman et al., 2014). The so-called mesocircuit hypothesis proposes that a loss of excitatory output from the central thalamus to diffuse cortical areas has a causative role in DOC (Schiff, 2008, 2010; Schiff and Posner, 2007). Such a loss is proposed to be caused by circuit dysfunction wherein inhibitory striatal output to the globus pallidus is lost, resulting in pallidal disinhibition and subsequent excessive inhibition of the thalamus. This mechanism is theorized to be driven by disinhibition of the globus pallidus interna specifically. Nevertheless, likely due to limitations in spatial resolution of the data, the above metabolic study (Fridman et al., 2014) considered the globus pallidus as a whole.

While recent functional neuroimaging studies seem to support the predictions of the mesocircuit model (see Giacino et al., 2014 for a review), it is unknown whether the hypothesized deafferentations are functional or anatomical. Structural impairments in thalamocortical and cortico-cortical fiber tracts of the DMN have been previously observed in DOC patients (Fernandez-Espejo et al., 2012). However, to our knowledge, the integrity of direct structural connections of the mesocircuit has not been investigated. A mechanistic understanding of the specific structural neural bases underlying DOC will be essential for the development of objective prognostic and diagnostic biomarkers.

The purpose of our study was to investigate structural integrity of the mesocircuit and its cortical projections in DOC patients, in order to lend structural support to observed differences in functional and metabolic brain activity in this poorly understood patient population. We used diffusion tensor imaging (DTI) tractography to reconstruct and

* Corresponding author at: School of Psychology, University of Birmingham, Birmingham, B15 2TT, UK.

http://dx.doi.org/10.1016/j.nicl.2015.11.004

assess the integrity of white matter connections between the nodes of the mesocircuit and several cortical regions *in vivo* in a group of DOC patients, as compared with healthy participants. DOC patients included those in the vegetative state (VS), minimally conscious state (MCS), and emerging-from-minimally conscious state (EMCS). We predicted that subcortico-subcortical connections would show less evidence of specific structural damage than subcortico-cortical and cortico-cortical connections in DOC patients. This prediction was based on several factors: 1) subcortico-cortical and cortico-cortical connections were previously shown to have evidence of significant structural damage in DOC patients (Fernandez-Espejo et al., 2012), 2) long range connections may be anatomically more susceptible to both diffuse axonal injury (Adams et al., 1982; Blumbergs et al., 1989; Johnson et al., 2013) and hypoxic–ischemic injury (Saab et al., 2013), and 3) the above described subcortical metabolic patterns (Fridman et al., 2014) suggested inhibitory pallidothalamic fibers (*i.e.* subcortico-subcortical) were intact.

2. Materials and methods

2.1. Participants

A convenience sample of 16 DOC patients participated in our study between February 2012 and November 2014. Inclusion criteria for the study were adult patients with a diagnosis of chronic DOC, or EMCS at the time of the study. The only exclusion criterion was unsuitability to enter the MRI environment. Independent functional and structural datasets from subsets of this cohort have been previously reported (Cruse et al., 2012; Fernandez-Espejo and Owen, 2013; Gibson et al., 2014; Naci and Owen, 2013; Naci et al., 2014). From these, 8 patients (4 VS patients, 3 MCS, and one EMCS) met the data quality criteria (see Section 2.3 below) and were included in the study. Patients were clinically assessed with repeated administrations of the Coma Recovery Scale—Revised (CRS-R; Giacino et al., 2004) over a 5 day visit to our center. The highest score achieved by each patient across the different examinations is included in Supplementary Information Table S1. Demographic and clinical data from the patients are summarized in Table 1. A group of 8 sex- (3 females) and age-matched healthy control subjects were also recruited for the study. The Health Sciences Research Ethics Board of The University of Western Ontario provided ethical approval for the study. All volunteers gave written informed consent and were paid for their participation in the experiment. Written assent was obtained from the legal guardian for all patients.

2.2. MRI acquisition

Diffusion-weighted images were acquired in a 3 T MRI scanner at the Centre for Functional and Metabolic Mapping (CFMM) at Robarts Research Institute (London, Canada). Patients were recruited over a time span of 2.5 years, during which the CFMM upgraded their 3 T scanner. Twelve participants (6 patients and 6 healthy controls) were scanned before the upgrade, in a Magnetom Trio system (Siemens, Erlangen, Germany), and the remaining four (2 patients and 2 healthy controls) were scanned in the new system: a Magnetom Prisma system (Siemens, Erlangen, Germany). This resulted in a balanced distribution of patients and healthy controls across the two different scanners. Similarly, the proportion between clinically conscious and clinically unconscious patients was also maintained across scanners. Diffusion-weighted images included sensitizing gradients applied in 64 non-collinear directions with a b-value = 700 s/mm^2, using an EPI sequence (Trio system: TR = 8700 ms, TE = 77 ms, voxel size = 2 × 2 × 2 mm, no gap, 77 slices; Prisma system: TR = 9600 ms, TE = 77 ms, voxel size = 2 × 2 × 2 mm, no gap, 76 slices). A high-resolution, T1-weighted, 3-dimensional magnetization prepared rapid acquisition gradient echo (MPRAGE) image was also acquired (Trio system: TR = 2300 ms, TE = 2.98 ms, inversion time = 900 ms, matrix size = 256 × 240, voxel size = 1 × 1 × 1 mm, flip angle = 9°; Prisma system: TR = 2300 ms, TE = 2.32 ms, inversion time = 900 ms, matrix size = 256 × 256, voxel size = 1 × 1 × 1 mm, flip angle = 8°).

2.3. DTI analyses

Motion related artifacts are a common methodological problem when working with DOC patients. Quality control of the data was performed by one of the authors (N.D.L.), who carefully inspected all diffusion-weighted raw images for the presence of motion related artifacts or macrostructural lesions or abnormalities in the regions of interest. Four DOC patients were excluded after visual inspection of DTI data revealed large artifacts due to excessive movement inside the scanner. An additional four DOC patients were excluded due to widespread and severe structural brain abnormalities that precluded accurate identification of either subcortical (n = 1), or both subcortical and cortical regions (n = 3) in the MRI data. All exclusions were made prior to fiber tracking and were made blinded to the clinical diagnosis of the patients.

Data preprocessing and analysis were performed using the FSL Diffusion Toolbox (http://fsl.fmrib.ox.ac.uk/fsl/fslwiki/), following a similar pipeline as Fernandez-Espejo et al. (2012) and Fernandez-Espejo et al. (2015). Pre-processing steps included eddy-current correction (Behrens et al., 2003a) and skull and non-brain tissue stripping using the Brain Extraction Tool (Smith, 2002). Fractional anisotropy (FA) maps were obtained using FSL Diffusion Toolbox (FDT; Behrens et al., 2003a). Diffusion modeling and probabilistic tractography were carried out using FDT. Fiber tracking between regions of interest (ROIs) was performed in native space for each subject (see Table 2 for summary of all fiber tracts), using FSL probtrackX (Jenkinson et al., 2012; Smith et al., 2004; Woolrich et al., 2009). Tracking was done in both directions between each set of two ROIs, and the resulting probability distribution was averaged and thresholded to 2% of the maximum intensity for each subject, in order to remove very-low probability paths. While there is currently no convention about the precise percentage, 2% has proven successful in previous studies of both healthy and pathological populations (Fernandez-Espejo et al., 2012; Sala-Llonch et al., 2010). The resulting tracts were visually inspected by one of the authors (N.D.L.) for correspondence with known anatomy and to ensure that our approach did not remove anatomically viable fibers.

Table 1
Summary of demographic and clinical characteristics of patients and controls.

Characteristic	Healthy controls	Patients	Statistic	P	Diagnostic categories			
					VS	MCS & EMCS	Statistic	P
Age, years, mean ± SD	26 ± 2	35 ± 11	t = −2.2	n.s.	31 ± 11	38 ± 10	t = 1.03	n.s.
Sex, M/F	5/3	5/3			3/1	2/2[a]		
Time post-ictus, days, mean ± SD		3523 ± 2914			2576 ± 3348	4472 ± 2492	t = 0.91	n.s.
VS/MCS/EMCS		4/3/1						
TBI/HBI		3/5			2/2	1[a]/3		
Scanner: Trio/Prisma	6/2	6/2			3/1	3/1[a]		

SD: standard deviation, VS: vegetative state, MCS: minimally conscious state, EMCS: emerging from minimally conscious state, TBI: traumatic brain injury, HBI: hypoxic–ischemic brain injury.
[a] Identifies the EMCS patient.

Table 2
Fiber tracts. A total of 12 left hemisphere, 12 right hemisphere and 1 midline fiber tract(s) were studied. 'Composite' fiber tracts in bold consisted of the fiber tracts listed below them. Stri: striatum, GP: globus pallidus, Tha: thalamus, FMC: frontal medial cortex, DLPFC: dorsolateral prefrontal cortex, PCu: precuneus, TPJ: temporoparietal junction.

Subcortico-subcortical fiber tract
Stri–GP
GP–Tha
Tha–Stri
Subcortico-cortical fiber tract
Tha–FMC
Stri–FMC
Tha-DLPFC
Stri–DLPFC
Tha–PCu
Stri–PCu
Lateralized cortico-cortical fiber tract
PCu–TPJ
FMC–DLPFC
TPJ–DLPFC
Midline cortico-cortical fiber tract
FMC–PCu

2.4. ROI masking

Regions of interest (ROIs) were obtained in a semi-automatic way and included subcortical structures and cortical areas. Subcortical structures were the main nodes of the anterior forebrain mesocircuit, as described in Schiff (2008): thalamus, globus pallidus (including both the internal and external subdivisions in a combined ROI), putamen, and caudate nucleus. The putamen and caudate nucleus were considered together as striatum to directly reflect the proposed schema of the anterior forebrain mesocircuit hypothesis (Schiff, 2008, 2010). The globus pallidus could not be reliably separated into internal and external segments due to limitations in anatomical resolution. All subcortical structures were defined individually in the left and right hemispheres and fiber tracking was performed to ipsilateral subcortical and cortical structures, as well as midline cortical structures, according to the schematic displayed in Fig. 3. Subcortical masks for each ROI were generated using the Harvard-Oxford Subcortical Structural Atlas (Frazier et al., 2005; Goldstein et al., 2007) on the MNI152 standard brain, and then unwarped to each subject's native space using the FSL linear registration tool, FLIRT (Jenkinson and Smith, 2001; Jenkinson et al., 2002), in a manner consistent with previous work (Fernandez-Espejo et al., 2012). A 2-step registration process within FLIRT (Jenkinson and

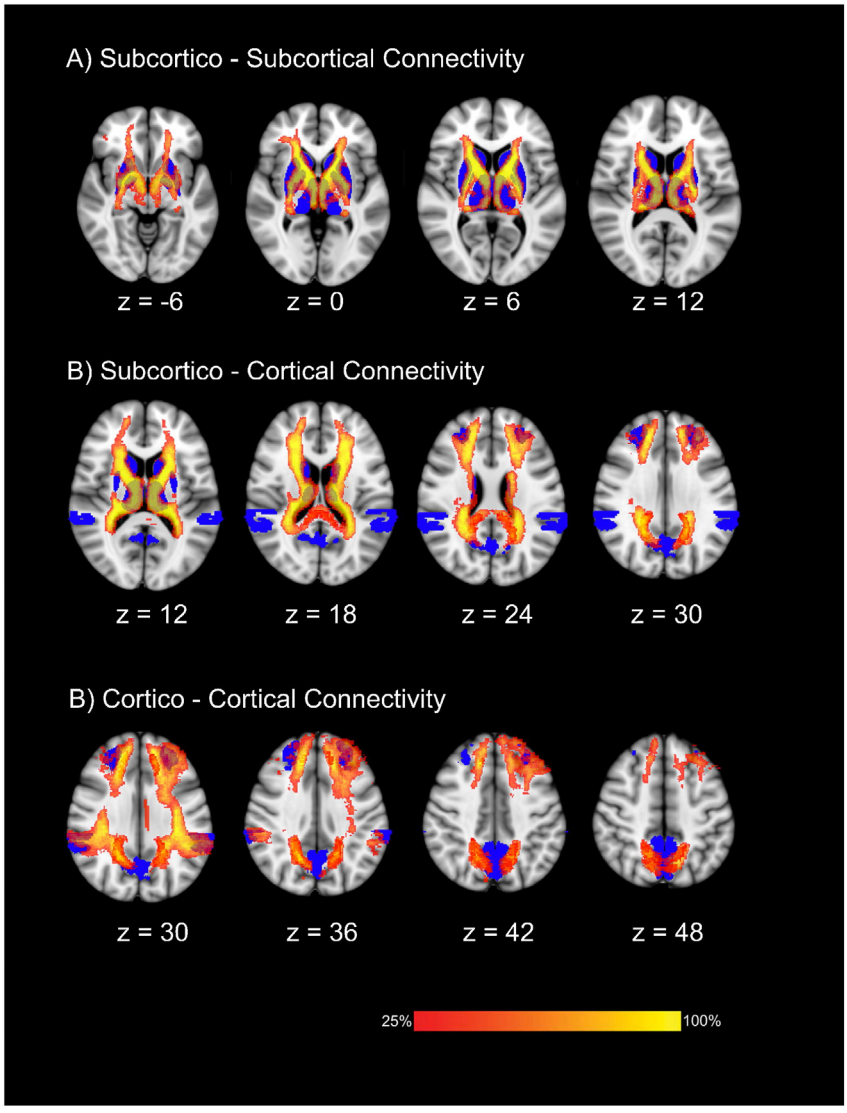

Fig. 1. Group probability maps of reconstructed tracts in healthy controls. Maps are thresholded at presence in at least 25% of healthy subjects. Regions of interest used for the tractography reconstruction are shown in blue. Images displayed in Montreal Neurological Institute standard stereotaxic space, and coordinates are provided for each slice.

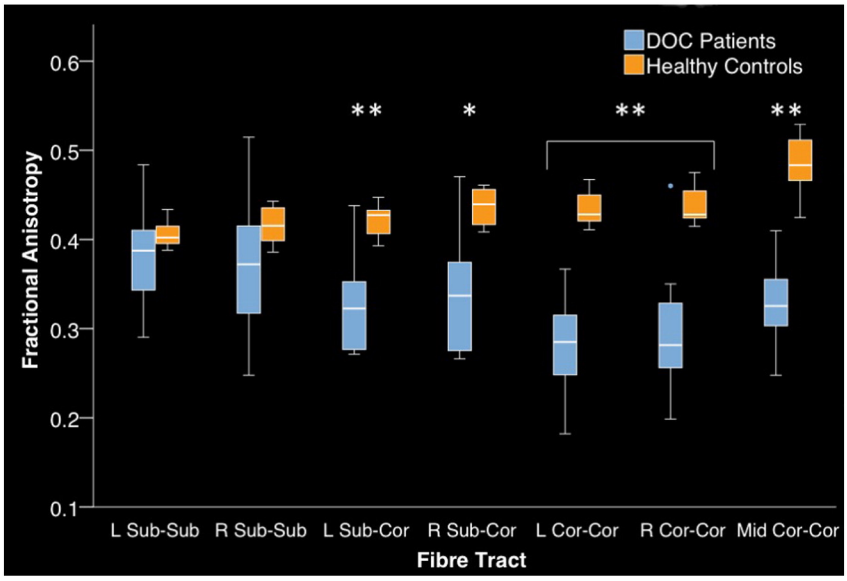

Fig. 2. Fractional anisotropy of composite fiber tracts in DOC patients and healthy controls. Middle line is median, lower box bound first quartile, upper box bound third quartile, whiskers 95% C.I., open circles outliers from C.I. Group main effect $^{*}p < 0.05$, $^{**}p < 0.01$. Sub: subcortical, Cor: cortical.

Smith, 2001; Jenkinson et al., 2002) was used with b = 0 image as low-resolution image, T1 as high resolution image, and the MNI152 1 mm template as the reference image. The inverse of the resulting transformation matrix was applied to each mask to unwarp it to native DTI space in each subject. After registration in native space, each mask was manually corrected in FSL View to ensure a close match with its anatomical boundaries. Because of the close proximity of these subcortical structures, care was taken to ensure that there was no overlap between the masks for each ROI in each subject (*e.g.* no overlap between globus pallidus and putamen masks). A stereotactic atlas of the basal ganglia and thalamus was used as qualitative visual aid and external reference to help define the appropriate boundaries of each ROI (Morel, 2007). For the thalamus, the transverse plane mean diffusivity (MD) map was used to define the thalamo-ventricular border (medial border of thalamus), and the transverse plane FA map was used to define the border between the thalamus and internal capsule (lateral border of

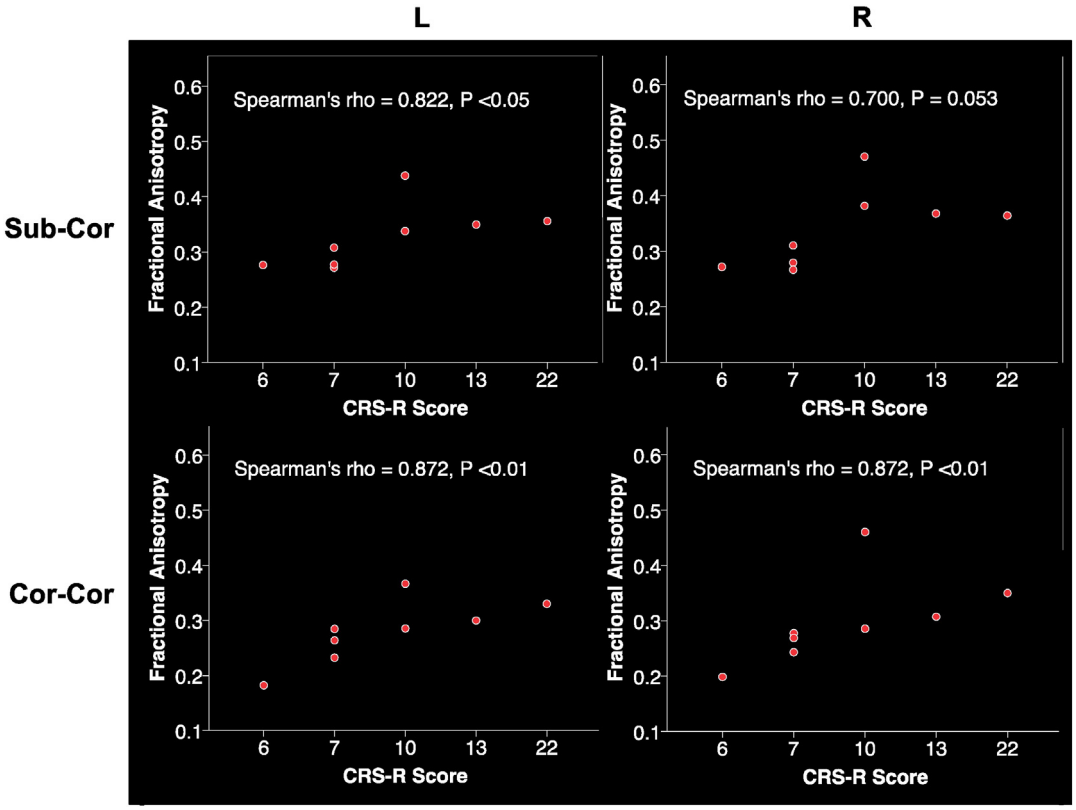

Fig. 3. Spearman correlations of CRS-R scores and composite fiber tract FA values for DOC patients. Sub-Cor: subcortico-cortical composite fiber tract, Cor-Cor: cortico-cortical composite fiber tract.

thalamus). After approximate segmentation in the transverse plane, the frontal plane FA map was used to define the shape of the thalamus more precisely. For the caudate, the transverse plane MD map was used to define the border between the caudate and the lateral ventricle, and the transverse plane FA map was used to define the border between the caudate and the internal capsule. The frontal plane FA map was used to define the shape of the caudate more precisely. MD and FA maps failed to provide adequate contrast for accurate delineation of anatomical boundaries of the putamen and globus pallidus. The T1 image acquired for each subject was registered to DTI space using FLIRT (Jenkinson and Smith, 2001; Jenkinson et al., 2002), and then visually inspected to ensure a correct alignment with the FA and MD maps. The boundaries of the unwarped putamen and globus pallidus ROIs were checked against both the registered T1 image and the FA map and manually corrected when necessary. This semi-automated method of subcortical ROI segmentation was chosen over fully automatic segmentation techniques because of the large anatomical variation found in DOC patient brains. Although automatic segmentation tools have been used previously for delineating the thalamus in DOC patients (Fernandez-Espejo et al., 2010; Lutkenhoff et al., 2015), the segmentation tools themselves are built on large collections of manually segmented regions (Patenaude et al., 2011). For consistency in our approaches for cortical and subcortical masking, we used the previously described semi-automatic method for both DOC patients and healthy controls.

While the mesocircuit model does not define specific cortical targets for its thalamic projections, we feel that cortical regions in the DMN are good candidates, due to the vast evidence implicating them in the neural basis of DOC (Cauda et al., 2009; Crone et al., 2013, 2015; Fernandez-Espejo et al., 2012; Fridman et al., 2014; Laureys et al., 1999; Soddu et al., 2012; Vanhaudenhuyse et al., 2010). Cortical ROIs thus included the precuneus (PCu), temporoparietal junction (TPJ), and frontal medial cortex (FMC). Additionally, we included the dorsolateral prefrontal cortex (DLPFC) as a potential cortical target for the following reasons: first, it is known to be systematically recruited by broad range of cognitive demands (Duncan and Owen, 2000); second, it has proven a key region for revealing covert awareness in behaviorally unresponsive patients (Naci and Owen, 2013; Naci et al., 2014); and finally, it has strong structural connections with the dorsomedial thalamic nucleus (Klein et al., 2010), which alongside the intralaminar nuclei comprises the central thalamus (Schiff, 2008), and is the thalamic nucleus that suffers from the most severe damage in VS patients (Fernandez-Espejo et al., 2010; Lutkenhoff et al., 2013; Maxwell et al., 2004, 2006).

Similarly to the above, where possible, cortical ROIs were generated from the Harvard-Oxford Cortical Atlas (Desikan et al., 2006; Makris et al., 2006), using a threshold of 50% in order to create a more conservative estimate. The only exception was the DLPFC which is not available in the FSL package. Due to the poorly defined structural boundaries of this area (Cieslik et al., 2013), we used the functional atlas generated by Shirer et al. (2011) (available here http://findlab.stanford.edu/functional_ROIs.html) to define this ROI. Specifically, the left and right DLPFC masks were manually extracted from their corresponding executive function networks.

The cortical masks were registered to each subject's native space using FLIRT, and following the same pipeline as for the subcortical masks above (Jenkinson and Smith, 2001; Jenkinson et al., 2002). The fitting of all masks was carefully inspected by author N.D.L., and manually corrected when needed.

To reduce multiple comparisons and to address our primary hypothesis, we created 3 'composite' masks for each hemisphere including subcortico-subcortical, subcortico-cortical, and lateralized cortico-cortical fiber tracts respectively for each subject (see Table 1 for individual tracts included in 'composite' fiber tracts). As the PCu and FMC are midline structures, the fiber tract connecting them was also considered midline and was analyzed separately, as part of the midline cortico-cortical mask. After analysis of composite fiber tracts, individual tracts were compared between DOC patients and healthy controls to extract more detailed patterns of impaired structural connectivity in DOC patients (see Section 2.5 for a detailed description of the statistical analysis).

Mean FA values for each pathway were calculated and used to quantify and compare the integrity of the identified paths. Patients for whom the specific pathway under investigation could not be identified with the tractography algorithm (see Table S2) were not included in the respective statistical analysis, as the inability to trace a pathway cannot be taken as evidence that the pathway does not exist and, thus, the interpretation of such a result is extremely challenging (Fernandez-Espejo et al., 2012; Johansen-Berg and Rushworth, 2009). In order to assess and control for the effects of global white matter damage, global white matter FA was calculated in controls and patients by thresholding the FA map to 0.2 and calculating the mean FA values of the remaining voxels above this threshold. White matter tissue is characterized by FA values above 0.2 (Mori and van Zijl, 2002) and thus such a threshold has been widely used to restrict the analysis of DTI derived maps to only white matter voxels in both healthy (Menzler et al., 2011) and pathological populations (Cherubini et al., 2007; Fernandez-Espejo et al., 2012; Hua et al., 2008; Palacios et al., 2011).

2.5. Statistical analysis

Statistical analyses were performed using IBM SPSS for Macintosh, Version 22. Shapiro–Wilk tests of normality were non-significant for all dependent measures (global white matter FA, fiber tract mean FA) in DOC patients and healthy controls, and thus parametric statistics were used.

Global white matter FA values were compared between DOC patients and healthy controls by means of one-way analysis of variance (ANOVA). Group comparisons of fiber tract FA values were performed using one-way analysis of covariance (ANCOVA) for non-lateralized paths, and repeated measures ANCOVA, with hemisphere as within subjects factor, for lateralized paths. Group (HC/DOC) served as the between-subjects factor. Linear correlations between each dependent variable and global FA, as well as scanner (Trio/Prisma), were performed in order to determine their inclusion as non-interest covariates in the ANCOVA. Only global FA showed significant effects in the studied tracts and thus was used as a covariate in both cases. The same statistical approach was employed for comparison of clinically conscious (MCS and EMCS) and clinically unconscious patients (VS). Additionally, in this case, the effect of time post ictus on the tracts was also tested. This yielded only non-significant results and thus time post-ictus was not included as a covariate in the ANCOVA. Subsequent comparisons of individual fiber tracts were done by one-way ANCOVA with global white matter FA as covariate. Significance was set *a priori* at $p < 0.05$. CRS-R scores were correlated to composite fiber tract FA values using Spearman's rank-order correlation, as CRS-R scores are ordinal variables.

3. Results

All fiber tracts were successfully identified in all healthy controls (see Fig. 1). The following fiber tracts were identified in all patients in both hemispheres: Stri–FMC, Striatum–Thalamus, Striatu–DLPFC, Thalamus–PCu, and TPJ–PCu. All other tracts were identified in at least 6 of 8 patients (See Table S2).

3.1. Differences between DOC patients and healthy controls

One-way ANOVA revealed significant differences in global white matter FA between DOC patients and healthy controls ($F_{1,14} = 4.662$, $p = 0.049$). This variable also correlated with our dependent variables (individual pathways FA) so it was included as a covariate in the

analysis of the individual pathways in order to control for the effect of widespread (*i.e.* nonspecific) white matter damage. Repeated measures ANCOVA on the lateralized composite fiber tracts revealed no significant effect of hemisphere on cortico-cortical fiber tract FA values. DOC patients had significantly lower FA values in these tracts (Fig. 2) ($F_{1,13} = 23.053$, $p < 0.001$), as well as midline cortico-cortical fiber tracts (*i.e.* PCu–FMC; $F_{1,11} = 21.155$, $p < 0.001$) as compared to controls. There was a significant effect of hemisphere on subcortico-subcortical and subcortico-cortical fiber tract FA values and therefore the left and right tracts were analyzed individually. Patients had significantly lower FA values in the left ($F_{1,13} = 11.594$, $p < 0.01$) and right ($F_{1,13} = 7.784$, $p < 0.05$) subcortico-cortical fiber tracts. In contrast, there was no significant effect of group on subcortico-subcortical fiber tract FA values. There was no significant group by hemisphere interaction in any fiber tracts.

3.2. Differences between clinically conscious and unconscious patients

There was no significant difference in time post-ictus ($t = 0.909$, $p = 0.399$) or age ($t = 1.03$, $p = 0.341$) between clinically conscious (MCS & EMCS) and clinically unconscious (VS) patients. There was a significant effect of hemisphere on subcortico-subcortical and subcortico-cortical composite fiber tract FA values, and these tracts were then analyzed by individual hemisphere. There were no significant differences between conscious and unconscious patients on FA values in subcortico-subcortical composite fiber tracts in the left ($F_{1,5} = 0.357$, $p > 0.05$) or right ($F_{1,5} = 0.353$, $p > 0.05$) hemisphere. In contrast, these groups significantly differed on FA values in subcortico-cortical fiber tracts in the right ($F_{1,5} = 12.607$, $p < 0.05$) hemisphere. Additionally, there was a trend towards significance in the left hemisphere ($F_{1,5} = 5.691$, $p = 0.063$). Finally, conscious and unconscious patients also differed in FA for lateralized cortico-cortical fiber tracts ($F_{1,6} = 7.340$, $p < 0.05$). No significant effects were identified for midline fiber tracts ($F_{1,4} = 6.062$, $p > 0.05$).

3.3. Correlation of fiber tract FA values with CRS-R score

CRS-R scores were significantly correlated with subcortico-cortical fiber tract FA values (see Fig. 2) in the left hemisphere (rho = 0.822, $p < 0.05$), and there was a trend of borderline significance in the right hemisphere (rho = 0.700, $p = 0.053$). CRS-R scores were significantly correlated with cortico-cortical fiber tract FA values (see Fig. 2) in the left (rho = 0.872, $p < 0.01$) and right (rho = 0.872, $p < 0.01$) hemispheres. There was no significant correlation between CRS-R scores and subcortico-subcortical fiber tract, midline cortico-cortical fiber tract or whole brain white matter FA values.

3.4. Individual tract analysis

Individual tract analysis revealed that all tracts involving the PCu had significantly lower FA in DOC patients relative to healthy controls (See Fig. 4). Other tracts with significantly lower FA in DOC patients included right hemisphere thalamus–FMC, bilateral DLPFC–FMC, left DLPFC–TPJ, and left Striatum–DLPFC. Left hemisphere striatum–globus pallidus had significantly higher FA in DOC patients. Detailed statistics are reported in Supplementary Information Table S2.

4. Discussion

Here, we provide the first report of the structural integrity of white matter fiber tracts connecting the nodes of the anterior forebrain mesocircuit and related cortical areas in DOC. We found evidence of significant impairment of both cortico-cortical and subcortico-cortical connections, which correlated with clinical severity as established by CRS-R scores. Moreover, clinically conscious patients differed from unconscious patients on subcortico-cortical and cortico-cortical fiber tract integrity, further supporting the importance of these connections in DOC.

4.1. Structural connectivity in the healthy brain

Twelve lateralized (total of 24) and one midline fiber tract(s) were found in all healthy control subjects. Reconstructed subcortico-subcortical fiber tracts matched well-defined striatopallidal, pallidothalamic and thalamostriatal connections of the classical basal ganglia loops (Alexander and Crutcher, 1990; Alexander et al., 1986). Reconstructed cortico-cortical fiber tracts within the default mode network corresponded to those previously found between homologous brain regions in tracer studies of non-human primates (Kobayashi and Amaral, 2003; Lavenex et al., 2002; Morris et al., 1999; Suzuki and Amaral, 1994), as well as DTI studies of humans (Fernandez-Espejo et al., 2012; Greicius et al., 2009). Fiber tracts reconstructed from the DLPFC were consistent with previous reports describing connections with other areas of the frontal cortex (Sallet et al., 2013), thalamus (Klein et al., 2010), striatum (Leh et al., 2007), and the inferior parietal lobule, a subregion of the TPJ (Mars et al., 2012). Finally, the identified subcortico-cortical fiber tracts followed well-established thalamocortical/corticothalamic and corticostriatal connections that have been found in tracer studies of non-human primates (Guillery and Sherman, 2002; Selemon and Goldman-Rakic, 1985), and validated in human DTI studies (Behrens et al., 2003b; Leh et al., 2007).

4.2. Structural impairments in DOC

Our results supported our prediction that subcortico-cortical and cortico-cortical projections related to the anterior forebrain mesocircuit would show more severe damage as compared to the fiber tracts interconnecting the subcortical nodes of the mesocircuit in DOC patients. Contrary to cortico-cortical and subcortico-cortical tracts, when widespread white matter damage was accounted for, DOC patients did not show significantly different FA values in subcortico-subcortical connections relative to controls. The specific mechanisms underlying the selectivity of this damage remain the subject of further investigation. Nevertheless, in non-traumatic patients one plausible hypothesis for the relative preservation of these subcortical fibers may relate to the higher metabolic demand for oxygen and nutrients that characterizes neurons with longer axons (Saab et al., 2013), which could make them more susceptible to hypoxic–ischemic injury. In traumatic patients, diffuse axonal injury (DAI; Meythaler et al., 2001) occurs predominantly in brain regions with adjacent tissues of different densities, such as the cerebral white–gray matter interface (Parizel et al., 1998). Longer-range subcortico-cortical and cortico-cortical fiber tracts may thus be particularly susceptible to this form of injury due to their topographical location. However, damage to subcortical white matter, basal ganglia and thalamus often appears in the context of both DAI (Adams et al., 1982, 2000; Gentry, 1994; Hesselink et al., 1988; Johnson et al., 2013) and hypoxic–ischemic brain injury (HBI; Adams et al., 2000), although those studies did not quantify whether the damage was affecting their subcortical or cortical projections. Given the small number of patients in each etiological category (TBI/HBI) we did not perform formal comparisons between them. It remains to be seen if etiological differences produce distinct patterns of white matter injury, and this may be a viable future direction of study.

Our findings provide a structural correlate to the main mechanism proposed by the mesocircuit hypothesis: loss of broad thalamic excitatory output as a result of a disinhibited and overactive globus pallidus (Schiff, 2010, 2008). This mechanism is predicated on the existence of inhibitory connections between the globus pallidus and thalamus (if they were structurally disconnected, the thalamus would be released from inhibition and would be expected to be more active). In identifying a relative preservation of pallidothalamic fibers in DOC patients, our results provide a structural underpinning for this model (Fridman et al., 2014). The mesocircuit model also suggests that a loss of striatal output

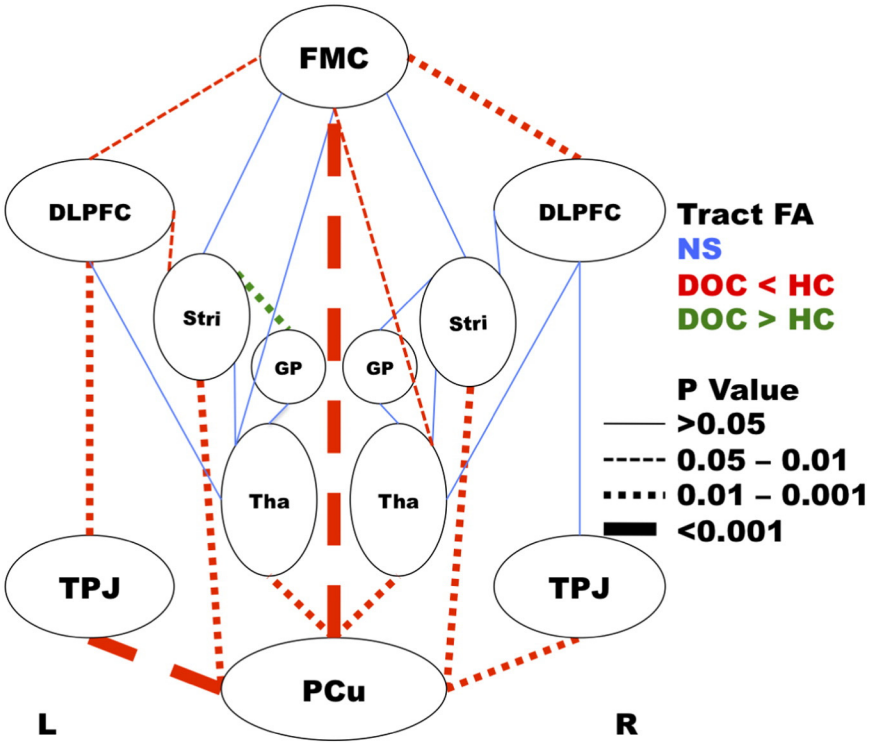

Fig. 4. Individual tract analysis comparing FA values between DOC patients and healthy controls. Blue solid lines represent fiber tracts with no significant differences. Red dashed lines represent fiber tracts with significantly lower FA in DOC patients relative to healthy controls. Green dashed lines represent fiber tracts with significantly higher FA in DOC patients relative to controls. Weight of line represents level of significance of difference between DOC patients and healthy controls. P value calculated by univariate analysis of covariance with whole brain white matter FA as covariate. DOC: disorders of consciousness, HC: healthy control, FMC: frontal medial cortex, DLPFC: dorsolateral prefrontal cortex, Stri: striatum, GP: globus pallidus, Tha: thalamus, TPJ: temporoparietal junction, PCu: precuneus, L: left hemisphere, R: right hemisphere. PCu–FMC tract is considered midline.

to the globus pallidus is the cause of pallidal disinhibition. The precise reasons for this proposed loss of striatal output are not known. Although we failed to identify significant damage in striatopallidal fibers in our DOC patients, very strong damage was found in some corticostriatal and thalamocortical/corticothalamic fibers. Specifically, we found evidence of significant structural damage to the connections between the PCu and both the thalamus and striatum (bilaterally) in DOC patients, perhaps suggesting a role for the Pcu in the dysregulation of the striatum and thalamus.

In addition to this, we also found evidence of damage in fiber tracts involving the DLPFC, which were more marked in the left hemisphere, in the DOC group. Functional engagement of this region has previously been used to demonstrate covert awareness in clinically vegetative patients (Naci and Owen, 2013; Naci et al., 2014). Interestingly, transcranial direct current stimulation of the left DLPFC has recently demonstrated some success in transiently improving signs of consciousness in MCS patients (Thibaut et al., 2014).

4.3. Role of the precuneus

The PCu (sometimes referred to as PCu/posterior cingulate cortex) is considered the main hub of the DMN (Cavanna and Trimble, 2006), and has shown specific functional impairments in DOC (Boly et al., 2009; Crone et al., 2015; Hannawi et al., 2015; Laureys et al., 2006; Vanhaudenhuyse et al., 2010). A recent study has provided further support to the role of the PCu in DOC by demonstrating that its function as main regulatory hub of the DMN (exerted with positive inputs and negative outputs) was lost in DOC patients (Crone et al., 2015). We have previously demonstrated structural disconnections of the PCu with the thalami, as well as the TPJ (Fernandez-Espejo et al., 2012). The results reported here expand those findings in providing evidence of significant damage in all the studied fiber tracts connecting the PCu with both cortical (*i.e.* TPJ, FMC) and subcortical (*i.e.* thalamus, striatum) areas. No other region in our study had such consistent evidence of damage. The mechanisms by which the PCu may be particularly susceptible to both TBI and HBI injury are not yet known. However, it is plausible that its long afferent and efferent axonal fibers, which connect it to distant cortical and subcortical targets (Cavanna and Trimble, 2006), along with its high metabolic activity at rest (Cavanna and Trimble, 2006), may make this structure especially vulnerable to the mechanisms of damage discussed above (*i.e.* those affecting long-range connections).

In any case, the structural disconnection of the PCu from the other nodes of the DMN could explain the lack of organized resting state activity previously described for DOC patients (see Hannawi et al., 2015 for a review). Furthermore, the PCu is widely connected to other cortical and subcortical regions (Cavanna and Trimble, 2006), and in addition to its role in the DMN, it is highly involved in visuo-spatial imagery and episodic memory retrieval networks (Cavanna and Trimble, 2006). Based on these somewhat opposed properties (Cavanna and Trimble, 2006; Crone et al., 2015), one could speculate that the PCu may act as a regulatory 'switch' to shift brain dynamics from inward-focused self-referential activity to task oriented activity. A recent large study of healthy adults has indeed found the PCu to have increased functional connectivity with the right fronto-parietal network (known to mediate external, or task-oriented awareness; Vanhaudenhuyse et al., 2011) during task performance, and with the DMN during rest (Utevsky et al., 2014). Interestingly, both networks have been related to clinical severity in severely brain injured patients, with locked-in patients having the greatest metabolic network activity and VS patients having the least (Thibaut et al., 2012). A complete structural disconnection of the PCu from other cortical and subcortical regions, as described here, may explain the (total or partial) reduction of its regulatory effect thereby impairing coordination of appropriate resting and non-resting state brain network dynamics. On this basis, it could be speculated that VS patients may be 'trapped' in a brain state that resembles neither resting

state nor goal directed activity due to the inability of the PCu to coordinate the inward focused state and the switch to outward focused brain states.

4.4. Conclusion

We propose a strong relationship between cortical areas in the DMN and the anterior forebrain mesocircuit in the neural basis of the DOC, which appears to be mediated by the PCu. Specifically, we showed that the subcortical mesocircuit is structurally intact, and the damage mainly affects projections to and from the PCu. This provides a structural framework to integrate theories based on mesocircuit dysfunctions (Giacino et al., 2014) with those pointing at the DMN (Hannawi et al., 2015) as causative of the lack of awareness in DOC patients.

5. Acknowledgments

This research was supported by generous funding from the Canadian Institutes of Health Research (Post-doctoral fellowship: D.F-E.; Operating Grant 0000032597: A.M.O.), James S. McDonnell Foundation (A.M.O.), Schulich Research Opportunities Program (N.D.L.), and the Canada Excellence Research Chairs Program (0000025914; A.M.O., D.F-E.). The funders had no role in study design, data collection and analysis, decision to publish, or preparation of the manuscript. We thank Natalie Osborne for assistance in healthy participant data collection.

Appendix A. Supplementary data

Supplementary data to this article can be found online at http://dx.doi.org/10.1016/j.nicl.2015.11.004.

References

Adams, J.H., Graham, D.I., Murray, L.S., Scott, G., 1982. Diffuse axonal injury due to nonmissile head injury in humans: an analysis of 45 cases. Ann. Neurol. 12, 557–563.
Adams, J.H., Graham, D.I., Jennett, B., 2000. The neuropathology of the vegetative state after an acute brain insult. Brain 123, 1327–1338. http://dx.doi.org/10.1093/brain/123.7.1327.
Alexander, G.E., Crutcher, M.D., 1990. Functional architecture of basal ganglia circuits: neural substrates of parallel processing. Trends Neurosci. 13, 266–271.
Alexander, G.E., DeLong, M.R., Strick, P.L., 1986. Parallel organization of functionally segregated circuits linking basal ganglia and cortex. Annu. Rev. Neurosci. 9, 357–381.
Behrens, T.E., Woolrich, M.W., Jenkinson, M., Johansen-Berg, H., Nunes, R.G., Clare, S., Matthews, P.M., Brady, J.M., Smith, S.M., 2003a. Characterization and propagation of uncertainty in diffusion-weighted MR imaging. Magn. Reson. Med. 50, 1077–1088. http://dx.doi.org/10.1002/mrm.10609.
Behrens, T.E.J., Johansen-Berg, H., Woolrich, M.W., Smith, S.M., Wheeler-Kingshott, C.A.M., Boulby, P.A., Barker, G.J., Sillery, E.L., Sheehan, K., Ciccarelli, O., 2003b. Non-invasive mapping of connections between human thalamus and cortex using diffusion imaging. Nat. Neurosci. 6, 750–757.
Blumbergs, P.C., Jones, N.R., North, J.B., 1989. Diffuse axonal injury in head trauma. J. Neurol. Neurosurg. Psychiatry 52, 838–841.
Boly, M., Tshibanda, L., Vanhaudenhuyse, A., Noirhomme, Q., Schnakers, C., Ledoux, D., Boveroux, P., Garweg, C., Lambermont, B., Phillips, C., Luxen, A., Moonen, G., Bassetti, C., Maquet, P., Laureys, S., 2009. Functional connectivity in the default network during resting state is preserved in a vegetative but not in a brain dead patient. Hum. Brain Mapp. 30, 2393–2400. http://dx.doi.org/10.1002/hbm.20672.
Cauda, F., Micon, B.M., Sacco, K., Duca, S., D'Agata, F., Geminiani, G., Canavero, S., 2009. Disrupted intrinsic functional connectivity in the vegetative state. J. Neurol. Neurosurg. Psychiatry 80, 429–431. http://dx.doi.org/10.1136/jnnp.2007.142349.
Cavanna, A.E., Trimble, M.R., 2006. The precuneus: a review of its functional anatomy and behavioural correlates. Brain 129, 564–583. http://dx.doi.org/10.1093/brain/awl004.
Cherubini, A., Luccichenti, G., Peran, P., Hagberg, G.E., Barba, C., Formisano, R., Sabatini, U., 2007. Multimodal fMRI tractography in normal subjects and in clinically recovered traumatic brain injury patients. Neuroimage 34, 1331–1341. http://dx.doi.org/10.1016/j.neuroimage.2006.11.024.
Cieslik, E.C., Zilles, K., Caspers, S., Roski, C., Kellermann, T.S., Jakobs, O., Langner, R., Laird, A.R., Fox, P.T., Eickhoff, S.B., 2013. Is there "one" DLPFC in cognitive action control? Evidence for heterogeneity from co-activation-based parcellation. Cereb. Cortex 23, 2677–2689. http://dx.doi.org/10.1093/cercor/bhs256.
Crone, J.S., Soddu, A., Holler, Y., Vanhaudenhuyse, A., Schurz, M., Bergmann, J., Schmid, E., Trinka, E., Laureys, S., Kronbichler, M., 2013. Altered network properties of the fronto-parietal network and the thalamus in impaired consciousness. NeuroImage Clin. 4, 240–248. http://dx.doi.org/10.1016/j.nicl.2013.12.005.
Crone, J.S., Schurz, M., Holler, Y., Bergmann, J., Monti, M., Schmid, E., Trinka, E., Kronbichler, M., 2015. Impaired consciousness is linked to changes in effective connectivity of the posterior cingulate cortex within the default mode network. Neuroimage 110, 101–109. http://dx.doi.org/10.1016/j. neuroimage .2015.01.037.
Cruse, D., Chennu, S., Fernandez-Espejo, D., Payne, W.L., Young, G.B., Owen, A.M., 2012. Detecting awareness in the vegetative state: electroencephalographic evidence for attempted movements to command. PLoS One 7, e49933. http://dx.doi.org/10.1371/journal.pone.0049933.
Desikan, R.S., Ségonne, F., Fischl, B., Quinn, B.T., Dickerson, B.C., Blacker, D., Buckner, R.L., Dale, A.M., Maguire, R.P., Hyman, B.T., Albert, M.S., Killiany, R.J., 2006. An automated labeling system for subdividing the human cerebral cortex on MRI scans into gyral based regions of interest. Neuroimage 31, 968–980. http://dx.doi.org/10.1016/j.neuroimage.2006.01.021.
Duncan, J., Owen, A.M., 2000. Common regions of the human frontal lobe recruited by diverse cognitive demands. Trends Neurosci. 23, 475–483.
Fernandez-Espejo, D., Owen, A.M., 2013. Detecting awareness after severe brain injury. Nat. Rev. 14, 801–809. http://dx.doi.org/10.1038/nrn3608.
Fernandez-Espejo, D., Junque, C., Bernabeu, M., Roig-Rovira, T., Vendrell, P., Mercader, J.M., 2010. Reductions of thalamic volume and regional shape changes in the vegetative and the minimally conscious states. J. Neurotrauma 27, 1187–1193. http://dx.doi.org/10.1089/neu.2010.1297.
Fernandez-Espejo, D., Soddu, A., Cruse, D., Palacios, E.M., Junque, C., Vanhaudenhuyse, A., Rivas, E., Newcombe, V., Menon, D.K., Pickard, J.D., Laureys, S., Owen, A.M., 2012. A role for the default mode network in the bases of disorders of consciousness. Ann. Neurol. 72, 335–343. http://dx.doi.org/10.1002/ana.23635.
Fernandez-Espejo, D., Bossit, S., Owen, A.M., 2015. I can only imagine; the overt versus covert paradox in the vegetative state. JAMA Neurol. 1–9. http://dx.doi.org/10.1001/jamaneurol.2015.2614.
Frazier, J.A., Chiu, S., Breeze, J.L., Makris, N., Lange, N., Kennedy, D.N., Herbert, M.R., Bent, E.K., Koneru, V.K., Dieterich, M.E., Hodge, S.M., Rauch, S.L., Grant, P.E., Cohen, B.M., Seidman, L.J., Caviness, V.S., Biederman, J., 2005. Structural brain magnetic resonance imaging of limbic and thalamic volumes in pediatric bipolar disorder. Am. J. Psychiatry 162, 1256–1265. http://dx.doi.org/10.1176/appi.ajp.162.7.1256.
Fridman, E.A., Beattie, B.J., Broft, A., Laureys, S., Schiff, N.D., 2014. Regional cerebral metabolic patterns demonstrate the role of anterior forebrain mesocircuit dysfunction in the severely injured brain. Proc. Natl. Acad. Sci. U. S. A. 111, 6473–6478. http://dx.doi.org/10.1073/pnas.1320969111.
Gentry, L.R., 1994. Imaging of closed head injury. Radiology 191, 1–17. http://dx.doi.org/10.1148/radiology.191.1.8134551.
Giacino, J.T., Kalmar, K., Whyte, J., 2004. The JFK Coma Recovery Scale—Revised: measurement characteristics and diagnostic utility. Arch. Phys. Med. Rehabil. 85, 2020–2029.
Giacino, J.T., Fins, J.J., Laureys, S., Schiff, N.D., 2014. Disorders of consciousness after acquired brain injury: the state of the science. Nat. Rev. 10, 99–114. http://dx.doi.org/10.1038/nrneurol.2013.279.
Gibson, R.M., Fernandez-Espejo, D., Gonzalez-Lara, L.E., Kwan, B.Y., Lee, D.H., Owen, A.M., Cruse, D., 2014. Multiple tasks and neuroimaging modalities increase the likelihood of detecting covert awareness in patients with disorders of consciousness. Front. Hum. Neurosci. 8, 950. http://dx.doi.org/10.3389/fnhum.2014.00950.
Goldstein, J.M., Seidman, L.J., Makris, N., Ahern, T., O'Brien, L.M., Caviness, V.S., Kennedy, D.N., Faraone, S.V., Tsuang, M.T., 2007. Hypothalamic abnormalities in schizophrenia: sex effects and genetic vulnerability. Biol. Psychiatry 61, 935–945. http://dx.doi.org/10.1016/j.biopsych.2006.06.027.
Greicius, M.D., Supekar, K., Menon, V., Dougherty, R.F., 2009. Resting-state functional connectivity reflects structural connectivity in the default mode network. Cereb. Cortex 19, 72–78. http://dx.doi.org/10.1093/cercor/bhn059.
Guillery, R.W., Sherman, S.M., 2002. Thalamic relay functions and their role in corticocortical communication: generalizations from the visual system. Neuron 33, 163–175.
Hannawi, Y., Lindquist, M.A., Caffo, B.S., Sair, H.I., Stevens, R.D., 2015. Resting brain activity in disorders of consciousness: a systematic review and meta-analysis. Neurology 84, 1272–1280. http://dx.doi.org/10.1212/WNL.0000000000001404.
Hesselink, J.R., Dowd, C.F., Healy, M.E., Hajek, P., Baker, L.L., Luerssen, T.G., 1988. MR imaging of brain contusions: a comparative study with CT. Am. J. Roentgenol. 150, 1133–1142. http://dx.doi.org/10.2214/ajr.150.5.1133.
Hua, K., Zhang, J., Wakana, S., Jiang, H., Li, X., Reich, D.S., Calabresi, P.A., Pekar, J.J., van Zijl, P.C., Mori, S., 2008. Tract probability maps in stereotaxic spaces: analyses of white matter anatomy and tract-specific quantification. Neuroimage 39, 336–347. http://dx.doi.org/10.1016/j.neuroimage.2007.07.053.
Jenkinson, M., Smith, S., 2001. A global optimisation method for robust affine registration of brain images. Med. Image Anal. 5, 143–156.
Jenkinson, M., Bannister, P., Brady, M., Smith, S., 2002. Improved optimization for the robust and accurate linear registration and motion correction of brain images. Neuroimage 17, 825–841.
Jenkinson, M., Beckmann, C.F., Behrens, T.E., Woolrich, M.W., Smith, S.M., 2012. Neuroimage 62, 782–790. http://dx.doi.org/10.1016/j.neuroimage.2011.09.015 (Fsl.).
Johansen-Berg, H., Rushworth, M.F., 2009. Using diffusion imaging to study human connectional anatomy. Annu. Rev. Neurosci. 32, 75–94. http://dx.doi.org/10.1146/annurev.neuro.051508.135735.
Johnson, V.E., Stewart, J.E., Begbie, F.D., Trojanowski, J.Q., Smith, D.H., Stewart, W., 2013. Inflammation and white matter degeneration persist for years after a single traumatic brain injury. Brain 136, 28–42. http://dx.doi.org/10.1093/brain/aws322.
Klein, J.C., Rushworth, M.F., Behrens, T.E., Mackay, C.E., de Crespigny, A.J., D'Arceuil, H., Johansen-Berg, H., 2010. Topography of connections between human prefrontal cortex and mediodorsal thalamus studied with diffusion tractography. Neuroimage 51, 555–564. http://dx.doi.org/10.1016/j. neuroimage .2010.02.062.
Kobayashi, Y., Amaral, D.G., 2003. Macaque monkey retrosplenial cortex: II. Cortical afferents. J. Comp. Neurol. 466, 48–79. http://dx.doi.org/10.1002/cne.10883.

Laureys, S., Goldman, S., Phillips, C., Van Bogaert, P., Aerts, J., Luxen, A., Franck, G., Maquet, P., 1999. Impaired effective cortical connectivity in vegetative state: preliminary investigation using PET. Neuroimage 9, 377–382. http://dx.doi.org/10.1006/nimg.1998.0414.

Laureys, S., Boly, M., Maquet, P., 2006. Tracking the recovery of consciousness from coma. J. Clin. Invest. 116, 1823–1825. http://dx.doi.org/10.1172/JCI29172.

Lavenex, P., Suzuki, W.A., Amaral, D.G., 2002. Perirhinal and parahippocampal cortices of the macaque monkey: projections to the neocortex. J. Comp. Neurol. 447, 394–420. http://dx.doi.org/10.1002/cne.10243.

Leh, S.E., Ptito, A., Chakravarty, M.M., Strafella, A.P., 2007. Fronto-striatal connections in the human brain: a probabilistic diffusion tractography study. Neurosci. Lett. 419, 113–118.

Lutkenhoff, E.S., McArthur, D.L., Hua, X., Thompson, P.M., Vespa, P.M., Monti, M.M., 2013. Thalamic atrophy in antero-medial and dorsal nuclei correlates with six-month outcome after severe brain injury. NeuroImage Clin. 3, 396–404. http://dx.doi.org/10.1016/j.nicl.2013.09.010.

Lutkenhoff, E.S., Chiang, J., Tshibanda, L., Kamau, E., Kirsch, M., Pickard, J.D., Laureys, S., Owen, A.M., Monti, M.M., 2015. Thalamic and extrathalamic mechanisms of consciousness after severe brain injury. Ann. Neurol. 78 (1), 68–76.

Makris, N., Goldstein, J.M., Kennedy, D., Hodge, S.M., Caviness, V.S., Faraone, S.V., Tsuang, M.T., Seidman, L.J., 2006. Decreased volume of left and total anterior insular lobule in schizophrenia. Schizophr. Res. 83, 155–171. http://dx.doi.org/10.1016/j.schres.2005.11.020.

Mars, R.B., Sallet, J., Schüffelgen, U., Jbabdi, S., Toni, I., Rushworth, M.F.S., 2012. Connectivity-based subdivisions of the human right "temporoparietal junction area": evidence for different areas participating in different cortical networks. Cereb. Cortex 22, 1894–1903. http://dx.doi.org/10.1093/cercor/bhr268.

Maxwell, W.L., Pennington, K., MacKinnon, M.A., Smith, D.H., McIntosh, T.K., Wilson, J.T.L., Graham, D.I., 2004. Differential responses in three thalamic nuclei in moderately disabled, severely disabled and vegetative patients after blunt head injury. Brain 127, 2470–2478. http://dx.doi.org/10.1093/brain/awh294.

Maxwell, W.L., MacKinnon, M.A., Smith, D.H., McIntosh, T.K., Graham, D.I., 2006. Thalamic nuclei after human blunt head injury. J. Neuropathol. Exp. Neurol. 65, 478–488. http://dx.doi.org/10.1097/01.jnen.0000229241.28619.75.

Menzler, K., Belke, M., Wehrmann, E., Krakow, K., Lengler, U., Jansen, A., Hamer, H.M., Oertel, W.H., Rosenow, F., Knake, S., 2011. Men and women are different: diffusion tensor imaging reveals sexual dimorphism in the microstructure of the thalamus, corpus callosum and cingulum. Neuroimage 54, 2557–2562. http://dx.doi.org/10.1016/j. neuroimage .2010.11.029.

Meythaler, J.M., Peduzzi, J.D., Eleftheriou, E., Novack, T.A., 2001. Current concepts: diffuse axonal injury-associated traumatic brain injury. Arch. Phys. Med. Rehabil. 82, 1461–1471.

Morel, A., 2007. Stereotactic Atlas of the Human Thalamus and Basal Ganglia. Informa Healthcare, New York.

Mori, S., van Zijl, P.C., 2002. Fiber tracking: principles and strategies — a technical review. NMR Biomed. 15, 468–480. http://dx.doi.org/10.1002/nbm.781.

Morris, R., Petrides, M., Pandya, D.N., 1999. Architecture and connections of retrosplenial area 30 in the rhesus monkey (*Macaca mulatta*). Eur. J. Neurosci. 11, 2506–2518. http://dx.doi.org/10.1046/j.1460-9568.1999.00672.x.

Naci, L., Owen, A.M., 2013. Making every word count for nonresponsive patients. JAMA Neurol. http://dx.doi.org/10.1001/jamaneurol.2013.3686.

Naci, L., Cusack, R., Anello, M., Owen, A.M., 2014. A common neural code for similar conscious experiences in different individuals. Proc. Natl. Acad. Sci. U. S. A. 111, 14277–14282. http://dx.doi.org/10.1073/pnas.1407007111.

Palacios, E.M., Fernandez-Espejo, D., Junque, C., Sanchez-Carrion, R., Roig, T., Tormos, J.M., Bargallo, N., Vendrell, P., 2011. Diffusion tensor imaging differences relate to memory deficits in diffuse traumatic brain injury. BMC Neurol. 11, 24. http://dx.doi.org/10.1186/1471-2377-11-24.

Parizel, P.M., Ozsarlak, Van Goethem, J.W., van den Hauwe, L., Dillen, C., Verlooy, J., Cosyns, P., De Schepper, A.M., 1998. Imaging findings in diffuse axonal injury after closed head trauma. Eur. Radiol. 8, 960–965.

Patenaude, B., Smith, S.M., Kennedy, D.N., Jenkinson, M., 2011. A Bayesian model of shape and appearance for subcortical brain segmentation. Neuroimage 56, 907–922. http://dx.doi.org/10.1016/j.neuroimage.2011.02.046.

Saab, A.S., Tzvetanova, I.D., Nave, K.A., 2013. The role of myelin and oligodendrocytes in axonal energy metabolism. Curr. Opin. Neurobiol. 23, 1065–1072. http://dx.doi.org/10.1016/j.conb.2013.09.008.

Sala-Llonch, R., Bosch, B., Arenaza-Urquijo, E.M., Rami, L., Bargallo, N., Junque, C., Molinuevo, J.L., Bartres-Faz, D., 2010. Greater default-mode network abnormalities compared to high order visual processing systems in amnestic mild cognitive impairment: an integrated multi-modal MRI study. J. Alzheimers. Dis. 22, 523–539. http://dx.doi.org/10.3233/JAD-2010-101038.

Sallet, J., Mars, R.B., Noonan, M.P., Neubert, F.X., Jbabdi, S., O'Reilly, J.X., Filippini, N., Thomas, A.G., Rushworth, M.F., 2013. The organization of dorsal frontal cortex in humans and macaques. J. Neurosci. 33, 12255–12274. http://dx.doi.org/10.1523/JNEUROSCI.5108-12.2013.

Schiff, N.D., 2008. Central thalamic contributions to arousal regulation and neurological disorders of consciousness. Ann. N. Y. Acad. Sci. 1129, 105–118. http://dx.doi.org/10.1196/annals.1417.029.

Schiff, N.D., 2010. Recovery of consciousness after brain injury: a mesocircuit hypothesis. Trends Neurosci. 33, 1–9. http://dx.doi.org/10.1016/j.tins.2009.11.002.

Schiff, N.D., Posner, J.B., 2007. Another "awakenings". Ann. Neurol. 62, 5–7.

Selemon, L.D., Goldman-Rakic, P.S., 1985. Longitudinal topography and interdigitation of corticostriatal projections in the rhesus monkey. J. Neurosci. 5, 776–794.

Shirer, W.R., Ryali, S., Rykhlevskaia, E., Menon, V., Greicius, M.D., 2011. Decoding subject-driven cognitive states with whole-brain connectivity patterns. Cereb. Cortex 22, 158–165. http://dx.doi.org/10.1093/cercor/bhr099.

Smith, S.M., 2002. Fast robust automated brain extraction. Hum. Brain Mapp. 17, 143–155. http://dx.doi.org/10.1002/hbm.10062.

Smith, S.M., Jenkinson, M., Woolrich, M.W., Beckmann, C.F., Behrens, T.E., Johansen-Berg, H., Bannister, P.R., De Luca, M., Drobnjak, I., Flitney, D.E., Niazy, R.K., Saunders, J., Vickers, J., Zhang, Y., De Stefano, N., Brady, J.M., Matthews, P.M., 2004. Advances in functional and structural MR image analysis and implementation as FSL. Neuroimage 23 (Suppl. 1), S208–S219. http://dx.doi.org/10.1016/j.neuroimage.2004.07.051.

Soddu, A., Vanhaudenhuyse, A., Bahri, M.A., Bruno, M.A., Boly, M., Demertzi, A., Tshibanda, J.F., Phillips, C., Stanziano, M., Ovadia-Caro, S., Nir, Y., Maquet, P., Papa, M., Malach, R., Laureys, S., Noirhomme, Q., 2012. Identifying the default-mode component in spatial IC analyses of patients with disorders of consciousness. Hum. Brain Mapp. 33, 778–796. http://dx.doi.org/10.1002/hbm.21249.

Suzuki, W.A., Amaral, D.G., 1994. Perirhinal and parahippocampal cortices of the macaque monkey: cortical afferents. J. Comp. Neurol. 350, 497–533.

Thibaut, A., Bruno, M.-A., Chatelle, C., Gosseries, O., Vanhaudenhuyse, A., Demertzi, A., Schnakers, C., Thonnard, M., Charland-Verville, V., Bernard, C., Bahri, M., Phillips, C., Boly, M., Hustinx, R., Laureys, S., 2012. Metabolic activity in external and internal awareness networks in severely brain-damaged patients. J. Rehabil. Med. 44, 487–494. http://dx.doi.org/10.2340/16501977-0940.

Thibaut, A., Bruno, M.A., Ledoux, D., Demertzi, A., Laureys, S., 2014. tDCS in patients with disorders of consciousness: sham-controlled randomized double-blind study. Neurology 82 (13), 1112–1118.

Utevsky, A.V., Smith, D.V., Huettel, S.a., 2014. Precuneus is a functional core of the default-mode network. J. Neurosci. 34, 932–940. http://dx.doi.org/10.1523/JNEUROSCI.4227-13.2014.

Vanhaudenhuyse, A., Noirhomme, Q., Tshibanda, L.J., Bruno, M.A., Boveroux, P., Schnakers, C., Soddu, A., Perlbarg, V., Ledoux, D., Brichant, J.F., Moonen, G., Maquet, P., Greicius, M.D., Laureys, S., Boly, M., 2010. Default network connectivity reflects the level of consciousness in non-communicative brain-damaged patients. Brain 133, 161–171. http://dx.doi.org/10.1093/brain/awp313.

Vanhaudenhuyse, A., Demertzi, A., Schabus, M., Noirhomme, Q., Bredart, S., Boly, M., Phillips, C., Soddu, A., Luxen, A., Moonen, G., Laureys, S., 2011. Two distinct neuronal networks mediate the awareness of environment and of self. J. Cogn. Neurosci. 23, 570–578. http://dx.doi.org/10.1162/jocn.2010.21488.

Woolrich, M.W., Jbabdi, S., Patenaude, B., Chappell, M., Makni, S., Behrens, T., Beckmann, C., Jenkinson, M., Smith, S.M., 2009. Bayesian analysis of neuroimaging data in FSL. Neuroimage 45, S173–S186. http://dx.doi.org/10.1016/j.neuroimage.2008.10.055.